RNA (2002), *8*:8–15. Cambridge University Press. Printed in the USA.

DOI: 10.1017.S1355838201010986

Structural and functional properties of the HIV-1 RNA–tRNA$_3^{Lys}$ primer complex annealed by the nucleocapsid protein: Comparison with the heat-annealed complex

FABIENNE BRULÉ,[1] ROLAND MARQUET,[1] LIWEI RONG,[2] MARK A. WAINBERG,[2] BERNARD P. ROQUES,[3] STUART F.J. LE GRICE,[4] BERNARD EHRESMANN,[1] and CHANTAL EHRESMANN[1]

[1]Unité Propre de Recherche 9002, Centre Nationale de la Recherche Scientifique, Institut de Biologie Moléculaire et Cellulaire, 67084 Strasbourg cedex, France
[2]McGill University AIDS Center, Lady Davis Institute–Jewish General Hospital, Montréal, Québec, H3T 1E2 Canada
[3]Unité Institut Nationale de la Santé et de la Recherche Médicale–Centre National de la Recherche Scientifique de Pharmacologie Moléculaire et Structurale, Unité de Recherche et de Formation des Sciences Pharmacologiques et Biologiques, 75270 Paris cedex, France
[4]Resistance Mechanism Laboratory, HIV Drug Resistance Program, National Cancer Institute-Frederick, Frederick, Maryland 21702-1206 USA

ABSTRACT

The conversion of the single-stranded RNA genome into double-stranded DNA by virus-coded reverse transcriptase (RT) is an essential step of the retrovirus life cycle. In human immunodeficiency virus type 1 (HIV-1), RT uses the cellular tRNA$_3^{Lys}$ to initiate the (–) strand DNA synthesis. Placement of the primer tRNA$_3^{Lys}$ involves binding of its 3′-terminal 18 nt to a complementary region of genomic RNA termed PBS. However, the PBS sequence is not the unique determinant of primer usage and additional contacts are important. This placement is believed to be achieved in vivo by the nucleocapsid domain of Gag or by the mature protein NCp. Up to now, structural information essentially arose from heat-annealed primer-template complexes (Isel et al., *J Mol Biol*, 1995, *247*:236–250; Isel et al., *EMBO J*, 1999, *18*:1038–1048). Here, we investigated the formation of the primer–template complex mediated by NCp and compared structural and functional properties of heat- and NCp-annealed complexes. We showed that both heat- and NCp-mediated procedures allow comparable high yields of annealing. Then, we investigated structural features of both kinds of complexes by enzymatic probing, and we compared their relative efficiency in (–) strong stop DNA synthesis. We did not find any significant differences between these complexes, suggesting that information derived from the heat-annealed complex can be transposed to the NCp-mediated complex and most likely to complexes formed in vivo.

Keywords: HIV-1; nucleocapsid protein; reverse transcription; tRNA annealing

INTRODUCTION

In human immunodeficiency virus type 1 (HIV-1), the cellular tRNA$_3^{Lys}$ binds to the primer binding site (PBS) on the genomic RNA serving as a primer for initiation of reverse transcription. Selective packaging of this host-derived tRNA requires the virus-coded Pr160$^{gag\text{-}pol}$ polyprotein (Mak et al., 1994). However, the PBS sequence is not the unique determinant of primer usage, as mutations of the PBS to match the 3′ end of tRNAs other than tRNA$_3^{Lys}$ dramatically reduce replication of the virus and lead to reversion to the wild-type PBS (Li et al., 1994; Das et al., 1995; Wakefield et al., 1995).

Thus, formation of the tRNA primer-viral RNA template binary complex and its recognition by reverse transcriptase is a crucial event for the initiation of reverse transcription. Up to now, structural and functional information on the primer–template complex essentially arose from complexes obtained by thermal annealing of tRNA$_3^{Lys}$ on viral RNA. Extensive chemical and enzymatic probing, in combination with computer modeling, revealed an unexpectedly complex structure

Reprint requests to: Chantal Ehresmann, UPR 9002, CNRS, Institut de Biologie Moléculaire et Cellulaire, 15 rue René Descartes, 67084 Strasbourg cedex, France; e-mail: Chantal.Ehresmann@ibmc.u-strasbg.fr.

(shown in Fig. 1) resulting from rearrangements of both molecules and leading to interactions between $tRNA_3^{Lys}$ and viral RNA, in addition to the PBS interaction (Isel et al., 1995, 1999), including an interaction between the U-rich anticodon loop of $tRNA_3^{Lys}$ and a conserved A-rich loop in U5 (helix 6C in Fig. 1). The latter interaction is supported by in vivo data that emphasized the essential role of the A-rich loop and the need for complementarity with the anticodon loop of the primer tRNA (Wakefield et al., 1996; Kang et al., 1997; Liang et al., 1997; Zhang et al., 1998). Furthermore, the binding and kinetic properties of reverse transcriptase markedly differ during the initiation step (i.e., addition of the first 6 nt) and subsequent elongation (Isel et al., 1996; Lanchy et al., 1996).

Because the tRNA primer and the U5-PBS region of the viral template are largely trapped in secondary structure (Baudin et al., 1993; Beerens et al., 2000), tRNA placement requires partial unfolding of both RNAs. In vivo, the viral nucleocapsid (NCp) domain of $p55^{gag}$ is believed to mediate primer/template annealing (Darlix et al., 1995; Feng et al., 1999). Although processing of $p55^{gag}$ is not required for the initial placement of tRNA onto the PBS (Huang et al., 1997), its optimal placement and initiation of reverse transcription appears to require mature NCp (Cen et al., 2000). The ability of mature NCp to anneal tRNA to the viral RNA at physiological temperature was demonstrated in vitro (Barat et al., 1989; de Rocquigny et al., 1992; Remy et al., 1998), and the biological relevance of this process is supported by results showing that the placement of tRNA is impeded in viruses with mutated NCp domains (Huang et al., 1998). Even though structural data obtained from the heat-annealed complex are supported by observations made in cell culture, the biological relevance of this complex has been questioned (Rong et al., 1998; Beerens & Berkhout, 2000). Moreover, no structural data on the complex formed in vivo or in vitro using NCp are currently available. To address this question, we performed a structural and functional comparison of heat-annealed and NCp-mediated primer–template complexes.

RESULTS

Optimal conditions for NCp-mediated annealing of $tRNA_3^{Lys}$ on viral RNA

A prerequisite to this study was quantitative and reproducible annealing of tRNA to its viral template, requir-

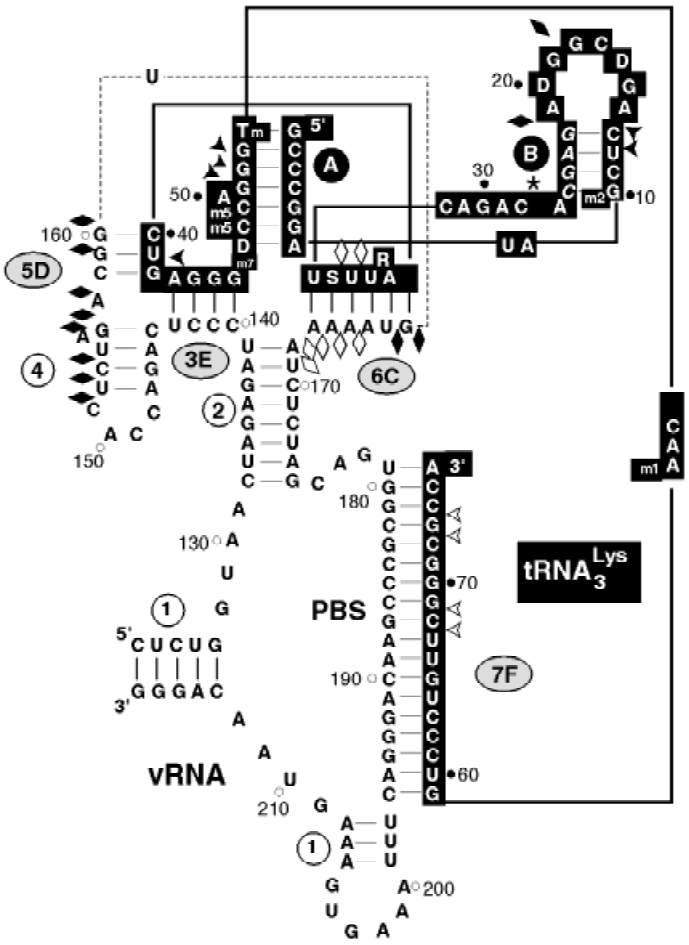

FIGURE 1. Secondary structure model of HIV-1 vRNA/$tRNA_3^{Lys}$ complex, deduced from previous enzymatic and chemical probing (Isel et al., 1995, 1999) and the probing experiments of this study. The tRNA sequence is in white on a black background. Helices are numbered according to Isel et al. (1995). Results of enzymatic probing obtained in this study are reported. Only cleavages differing in the binary complexes as compared to the free tRNA (or vRNA) are indicated. Cuts are indicated by diamonds (RNase ONE) and arrowheads (RNA V1). Increased and decreased cleavages are indicated by black and white symbols, respectively. An increased nonenzymatic cut present in the NCp-annealed and not in the heat-annealed complex is marked by an asterisk.

ing optimization of the NCp-mediated hybridization conditions. Indeed, various experimental procedures were reported in the literature, yielding quite different annealing efficiencies. Because a possible cause of the observed discrepancies is the presence or absence of a purification step after RNA template transcription, we tested different usual components of the transcription medium that may interfere with the annealing process, starting with a purified RNA template. We used natural 3′-end-labeled $tRNA_3^{Lys}$ primer, allowing a quantitative evaluation of bound tRNA.

A first result that emerged from this study is that the presence of 1 mM spermidine and 8 mM NTPs considerably improved the quality of the gel mobility shift assays (Fig. 2B and data not shown). These components do not interfere with the annealing efficiency (see following section), but rather reduce the formation of aggregates that are frequently observed in their absence. Therefore, in the following, spermidine and NTPS were added in gel shift experiments and omitted in probing and strong-stop DNA synthesis experiments.

As shown in Figure 2B, formation of the binary complex increased as a function of $NCp_{(1–72)}$ concentration, and a plateau was reached at one NCp per 5 nt (Fig. 2C). A NCp:RNA ratio of one NCp per 7.5 nt was chosen in the following experiments. On the other hand, the heat-annealing procedure yielded a complete annealing and the resulting complex migrated at the same position as the NCp-annealed complex (Fig. 2A).

Unexpectedly, we found that DTT, a usual component of transcription and annealing buffers, reduced formation of the NCp-annealed complex in a concentration dependent manner (results not shown). Indeed, DTT was found to reduce the annealing activity to about 20% at 0.05 mM (a 12.5-fold excess of DTT over NCp under our experimental conditions), and complete inhibition was reached at 0.2 mM. As a consequence, the addition of RNasin® also exerted an inhibitory effect, due to the presence of DTT (8 mM) in its storage buffer (results not shown).

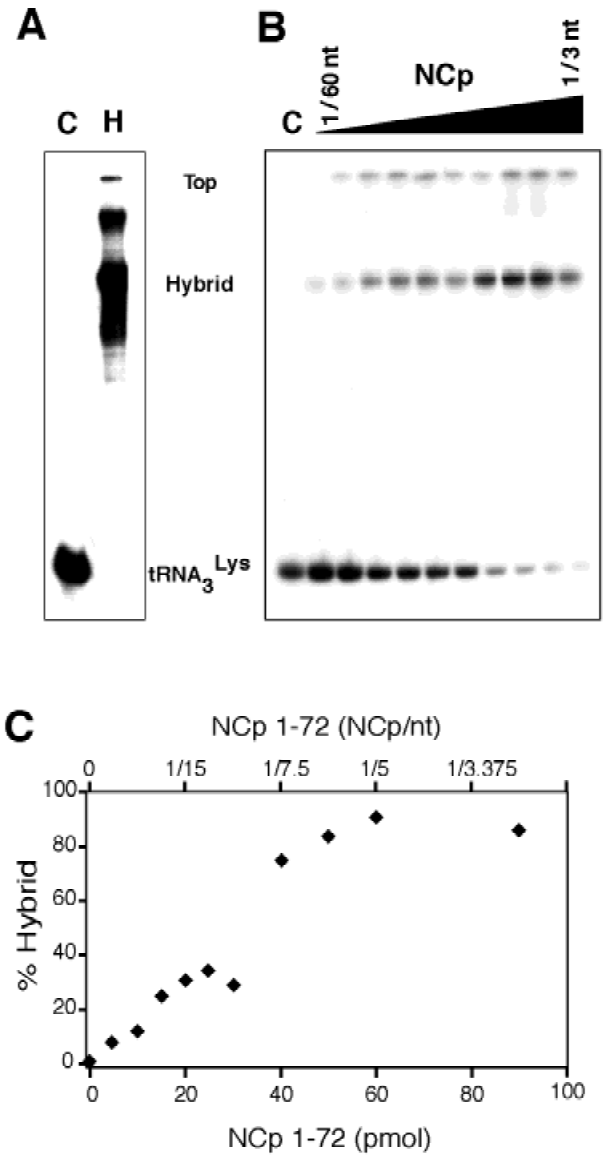

FIGURE 2. Band shift assays showing heat- and $NCp_{(1–72)}$-mediated annealing of 3′-end-labeled $tRNA_3^{Lys}$ on HIV-1 RNA. Free $tRNA_3^{Lys}$, hybrid ($tRNA4_3^{Lys}$/viral RNA binary complex) and the top of the gel are indicated. **A**: Free tRNA (lane C) and heat-annealed complex (lane H). **B**: Formation of the NCp-annealed complex, as a function of NCp concentration. $tRNA_3^{Lys}$ and viral RNA were incubated in the absence (lane C) or presence of 5–90 pmol NCp, corresponding to the following NCp per nucleotide ratio: 1/60; 1/30; 1/20; 1/15; 1/12.5; 1/10; 1/7.5; 1/6.25; 1/5, and 1/3. Note that the gel in **B** is more exposed than the gel in **A**. **C**: Quantification of the gel shown in **B**.

Probing of $tRNA_3^{Lys}$ and viral RNA in heat- and NCp7-annealed complexes

Next, we used structure-specific RNases to probe $tRNA_3^{Lys}$ and viral RNA, either free or engaged in the NCp- or heat-annealed complexes. We used RNase ONE™ and RNase V1, specific for unpaired and paired nucleotides, respectively. After annealing, both complexes were submitted to the same protocol, including the proteinase K and phenol/chloroform treatment used to remove NCp. Cleavages were detected directly on 3′-end-labeled tRNA, and following primer extension for the viral RNA, as previously described (Isel et al., 1995).

The accessibility pattern of bound tRNA (Fig. 3), either annealed by heat or NCp, is fully consistent with the proposed secondary structure model of Figure 1 (Isel et al., 1995, 1999). As expected, G18 and A21 in the D loop became increasingly susceptible to RNase ONE upon complex formation, due to disruption of the ternary interactions between the D- and TΔC-loops of the tRNA during formation of the binary complex. Concomitantly, U12 and C13 in the D stem became more accessible to RNase V1, whereas the accessibility of the 3′ part of the tRNA engaged in the PBS helix was strongly decreased (nt 67 to 73). The latter observation

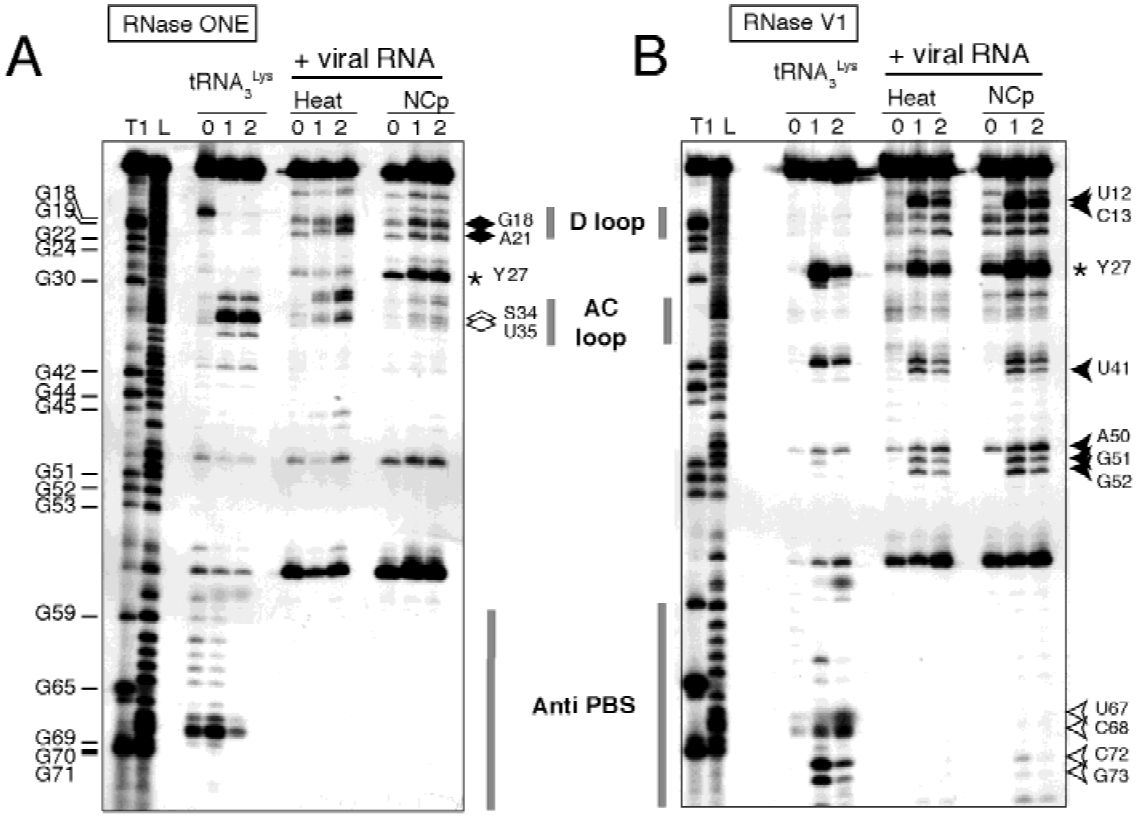

FIGURE 3. Enzymatic probing of free $tRNA_3^{Lys}$ and $tRNA_3^{Lys}$/vRNA complexes formed either by heat annealing or by NCp. Lanes 0 are controls incubated in the absence of RNases. **A**: Probing with RNase ONE: incubation with 0.05 U of RNase at 20 °C for 10 (lane 1) and 15 min (lane 2). **B**: Probing with RNase V1, same conditions as above. Cleavages specifically observed in free tRNA or in the binary complex are indicated. Lanes T1 and L refer to nuclease T1 sequencing and alkaline ladder, respectively. The anticodon and D loops, and the anti-PBS region are indicated. The nonenzymatic cut increase in the NCp-annealed complex is indicated by an asterisk. A band compression is observed at G70–G71.

is in keeping with the known inability of RNase V1 to cleave efficiently in the middle of very long and regular helices (Moine et al., 1997). The absence of these cleavages is a strong indication for the disappearance of the native form of the primer tRNA, suggesting complete commitment of tRNA in helix 7B. This interpretation is supported by the fact that incubation of tRNA with NCp in absence of RNA template did not induce any change in its accessibility profile (not shown). Otherwise, the increased accessibility of U41 to RNase V1 (Fig. 3B) was due to formation of intermolecular helix 5D (Fig. 1), whereas the increased cleavages at A50, G51, and G52 reflected the newly formed intramolecular helix A. Finally, a clear protection of nt S34 and U35 (in the anticodon loop) to RNase ONE was observed (Fig. 3A), reflecting the interaction with the viral A-loop (helix 6C). The only difference between heat- and NCp-annealed complexes concerned the presence of a nonenzymatic cleavage at position 27 that was reproducibly observed in the NCp-promoted complex and not in the heat-annealed one (Fig. 3A,B), although both complexes were treated under similar conditions, As a possible explanation, some of the peptides generated by NCp proteolysis (and absent in the heat-annealed duplex) might account for an increased fragility of this phosphodiester bound.

Consistent with these observations, A164 to A167 in the A-loop were clearly protected from RNase ONE in the viral RNA (Fig. 4). Strikingly, nt U154 to G162 appeared to be more susceptible to RNase ONE in the binary complex than to RNase T2 or *Neurospora crassa* nuclease previously used by Isel et al. (1995, 1999) to study the heat-annealed complex, most likely reflecting the small size and a higher sensitivity of this enzyme to irregularities of the secondary structure.

(–) strong stop DNA synthesis

Finally, we compared the relative efficiency of NCp- and heat-annealed complexes in (–) strong stop DNA synthesis. NCp-mediated annealing was conducted with both $NCp_{(1–72)}$ and $NCp_{(1–55)}$. The binary complexes were incubated with RT and reverse transcription was initiated by addition of the four dNTPs and terminated at different time intervals with formamide and 50 mM EDTA. No significant difference was observed between the kinetics of reverse transcription in the three types of complexes (Fig. 5A). Quantitative analysis of the gels

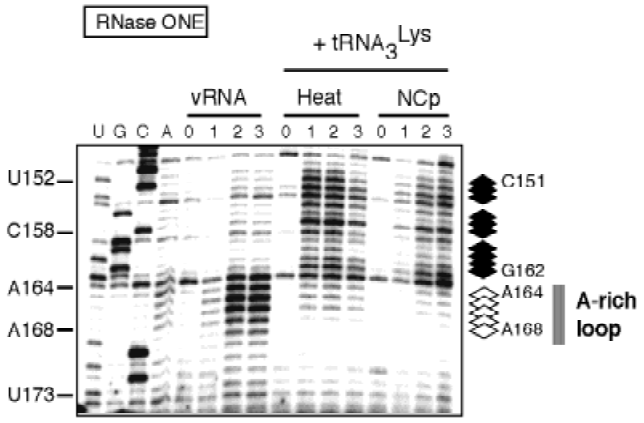

FIGURE 4. Probing with RNase ONE of free vRNA and vRNA/tRNA$_3^{Lys}$ complexes formed either by heat annealing or by NCp protein. Lanes 0 are controls incubated in the absence of RNase. Lanes 1, 2, and 3 correspond to incubation with 0.05 U of RNase ONE for 5, 10, and 15 min, respectively. Cleavages specifically observed in free tRNA or in the binary complex are indicated (as in Fig. 1). Sequencing lanes (U, G, C, and A) were run in parallel. The A-rich loop is indicated.

indicated that the elongation rate was very similar in both NCp-mediated and in heat-annealed complexes, with the same amount of product formed after 5 min (Fig. 5B). Furthermore, intermediate pausing products displayed a similar time-dependent profile. In particular, pauses observed for the addition of the first 6 nt were characteristic of the slow initiation phase previously described (Isel et al., 1996; Lanchy et al., 1996).

DISCUSSION

Data found in the literature on the efficiency of NCp-mediated annealing of the primer tRNA$_3^{Lys}$ on the viral RNA template has been so far subject to high variations, mostly linked to differences in experimental protocols, state of NCp, and uncertainties about estimation of annealing yield. For example, data ranged from a total absence of tRNA annealing at 37 °C (Beerens & Berkhout, 2000) to almost complete annealing (Chan & Musier-Forsyth, 1997). Otherwise, heat-annealing protocols substantially differ, resulting also in variable annealing efficiencies. Therefore, a reliable comparison between the two processes was made very difficult. Here, we could obtain high yield of annealing of natural tRNA$_3^{Lys}$ to viral RNA using both procedures (Fig. 2), thus enabling a correct structural and functional comparison of both complexes.

Unexpectedly, we found that DTT has an inhibitory effect on the NCp-mediated annealing process. The presence of DTT (or RNasin as an undesired source of DTT) in annealing buffers used in the literature appeared to be a hardly appreciable parameter. In most cases, DTT was clearly not a constituent of the annealing buffer; however, noncontrolled amounts of DTT could be introduced when purification of the template RNA after transcription was omitted. However, no clear explanation obviously accounts for the inhibitory effect of DTT. One possible explanation could be related to the strong chelating properties of DTT, which has been described to form specific and very stable polymeric and monomeric complexes with metal ions including Zn (II), using both of its sulfur donors (Krezel et al., 2001). However, the high affinity of the NCp zinc fingers ($K_A \sim 10^{13}$ M^{-1}; Mély et al., 1991) renders unlikely a possible displacement of zinc by DTT. An alternative explanation could be linked to the presence of DTT oxidation products or contaminant. It should be stressed that the nature of the oxidation products appeared to depend on the source of DTT (Krezel et al., 2001).

The present results unambiguously showed that placement of tRNA$_3^{Lys}$ by the mature NCp yields a primer template with the same structural and functional characteristics as the heat-annealed complex. This contradicts previous reports suggesting differences between these complexes (Rong et al., 1998; Beerens & Berkhout, 2000). However, it should be stressed that in the experiments conducted by the latter authors, NCp-mediated annealing was obtained at high temperature (60 or 85 °C), because they failed to achieve annealing at 37 °C. Our finding is consistent with the fact that thermal denaturation/renaturation promotes the most thermodynamically stable conformation. On the other hand, NCp was shown to possess nucleic acid chaperone activities in a wide variety of assays by favoring annealing of complementary sequences and allowing formation of alternate secondary structures (Herschlag, 1995; Rein et al., 1998). The zinc fingers were proposed to be required for chaperone functions involving complex nucleic acid rearrangements in (−)- and (+)-strand transfer (Guo et al., 2000) and in single molecule stretching experiments (Williams et al., 2001). Here, NCp promotes conformational rearrangements into optimal base-paired structures, most likely by lowering the energy barrier for breakage and reformation of base pairs. A first insight into the annealing mechanism was revealed by FRET measurements, showing that NCp does not unwind the acceptor stem of an in vitro synthesized tRNA primer in the absence of the template RNA (Chan et al., 1999). This is consistent with our own observation indicating that the accessibility of natural tRNA$_3^{Lys}$ was unaffected by incubation with NCp in absence of acceptor RNA. In addition, the same distance was measured between the two ends of the tRNA in both heat- and NCp-mediated annealing in the FRET experiments in the presence of the template RNA (Chan et al., 1999). More recently, it was shown that NCp reduces the cooperativity of the helix-coiled transition of double-stranded DNA structures. Thus, NCp is supposed to cause continuous melting and reannealing so that nucleic acids are able to rapidly sample conformations allowing them to find the most stable state (Williams et al., 2001).

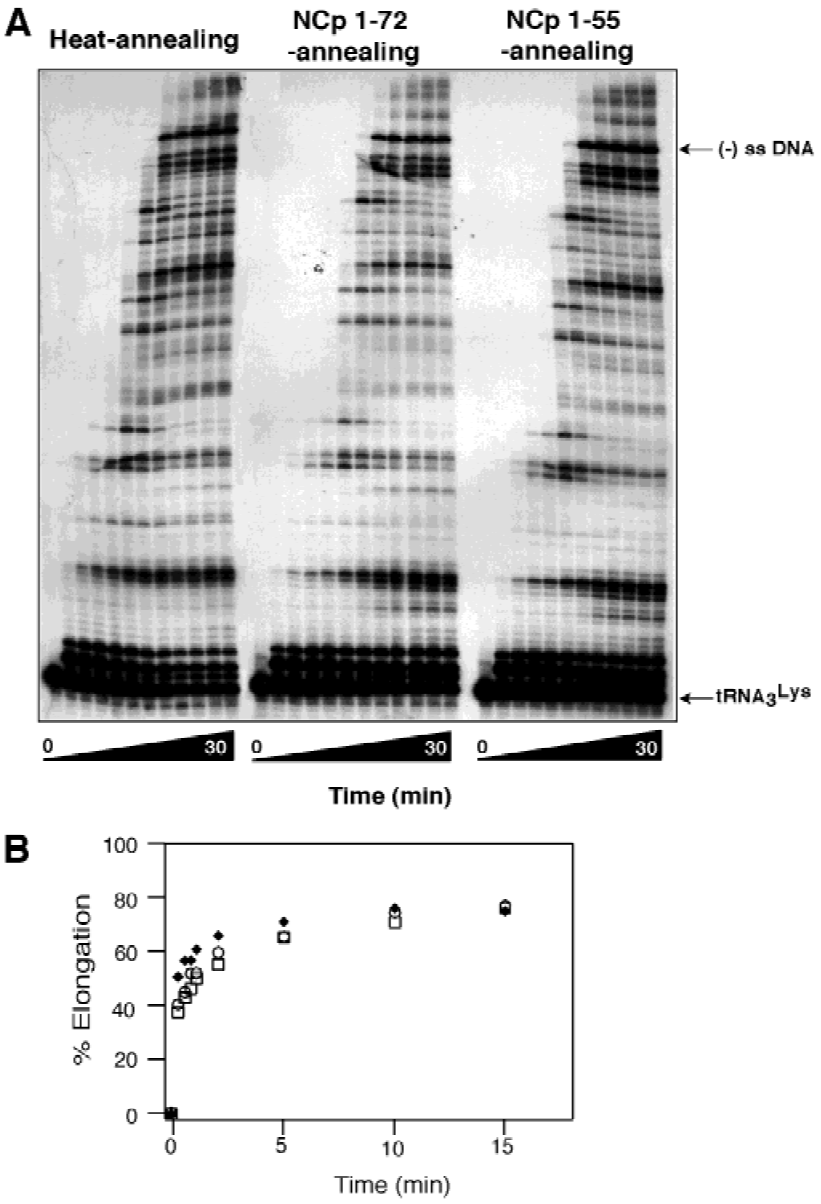

FIGURE 5. Minus strong stop DNA synthesis using NCp- and heat-annealed primer–template complexes. Two forms of NCp were used ($NCp_{(1–72)}$ and $NCp_{(1–55)}$) at a NCp:RNA ratio of 1:7.5 and 1:5.5 nt, respectively. The resulting primer/template complexes were treated as indicated in the text. Aliquots were analyzed at intervals of 0 s, 15 s, 30 s, 45 s, 1 min, 2.5 min, 5 min, 10 min, 15 min, 20 min, 25 min, and 30 min. **A**: Autoradiograph of the gel showing the time courses of labeled $tRNA_3^{Lys}$ extension. Unextended $tRNA_3^{Lys}$ and (−) strong stop DNA are indicated. Bands running slower than the (−) strong stop DNA correspond to self-priming products. **B**: Quantitative analysis of the formation of (−) strong stop DNA synthesis as a function of time (during the first 15 min): heat-annealed complex (filled circles), $NCp_{(1–72)}$- and $NCp_{(1–55)}$-annealed complexes (open circles and squares, respectively). For each time, the percentage of elongation was calculated as: $100 \times [Ep/(\text{tRNA} + Ep)]$, tRNA being the unextended tRNA and Ep the sum of elongation products.

Taken together, these findings strongly suggest that information derived from the heat-annealed complex can be transposed to the NCp-mediated complex and likely to the complex formed in vivo.

MATERIALS AND METHODS

RNA template, primers, and proteins

The plasmid used to obtain the RNA template corresponding to nt 1–311 of $HIV\text{-}1_{Mal}$ is described in Marquet et al. (1991). The RNA was synthesized in vitro by transcription with T7 RNA polymerase in the transcription buffer (40 mM Tris HCl, pH 8.0, 50 mM NaCl, 15 mM $MgCl_2$, 5 mM DTE, 1 U/μL RNasin,1 mM spermidine, 0.05% Triton, 0.05 mg/mL BSA) in the presence of 4 mM NTP, at 37 °C for 1 h. After treatment with RNase-free DNase I (Appligene), phenol-chloroform extraction and ethanol precipitation, the RNA transcript was purified on a Bio-Sil TSK 250 (Biorad) column using a FPLC (Pharmacia) system in 200 mM sodium acetate, pH 6.5, 1% methanol. After concentration in Centricon 10 (Amicon), the RNA was precipitated with ethanol and resuspended in water prior to use. The natural $tRNA_3^{Lys}$ from beef liver was purified and labeled at its 3′ end as described (Bénas et al., 2000). NCp (72 or 55 residues) was chemically synthesized (de Rocquigny et al., 1991). The wild-type HIV-1 RT was purified according to Le Grice and Grueninger-Leitch (1990). Deoxyribonucleotide primer (IBA-NAPS, Göttingen) was 5′-end labeled using [^{32}P]-ATP (NEN, Boston) and T4 polynucleotide kinase (New England Biolabs, Beverly, MA).

tRNA annealing

Heat-annealing of $tRNA_3^{Lys}$ to viral RNA was essentially performed as described (Isel et al., 1993). Briefly, viral RNA and $tRNA_3^{Lys}$ were incubated in water for 2 min at 90 °C, cooled on ice, and incubated 20 min at 70 °C in the appropriate buffer. The NCp-annealed complex was formed by incubating the viral RNA and the primer tRNA with NCp at 37°C for 30 min, in 10 μL of annealing buffer (50 mM Tris-HCl, pH 7.2, 50 mM KCl, and 5 mM $MgCl_2$). Individual components, such as NTPs, spermidine, DTT (Sigma), and RNasin (Promega), were added to the annealing buffer as specified in the text. NCp was removed by hydrolysis with proteinase K (1 mg/mL final concentration for 30 min at 37°C), followed by phenol/chloroform extraction and precipitation with 0.4 M ammonium acetate and an equal volume of isopropanol.

The annealing of $tRNA_3^{Lys}$ to viral RNA was analyzed by gel shift assays. In these experiments, 0.3 pmol of $tRNA_3^{Lys}$ (containing 10,000 cpm of 3′-end-labeled tRNA) and 1 pmol of viral RNA were used. The samples were analyzed by polyacrylamide (8%) gel electrophoresis under nondenaturing conditions. The products were quantified with a BioImager BAS 2000 (Fuji).

Enzymatic probing of RNAs

Heat- and $NCp_{(1–72)}$-mediated annealing were as described above. The heat-annealed complex was submitted to the same proteinase K and phenol/chloroform treatment as the NCp-annealed complex. The two complexes were then incubated at 20 °C for 10 min in 50 mM sodium cacodylate, pH 7.5, 300 mM KCl, and 5 mM $MgCl_2$ before RNase hydrolysis. tRNA and viral RNA probing were done on binary complexes formed with either 0.3 pmol of 3′-end-labeled tRNA $tRNA_3^{Lys}$ and 1 pmol of viral RNA, or 1 pmol tRNA and 0.3 pmol viral RNA, respectively. Hydrolysis with RNase ONE (Promega) and RNase V1 (Pharmacia) was with 0.05 U of enzyme, for 10 and 15 min at 20 °C. After incubation, the RNAs were submitted to phenol/chloroform extraction and ethanol precipitation. For tRNA probing, the samples were directly analyzed by electrophoresis on 15% denaturing polyacrylamide gels (Isel et al., 1995). As for enzymatic viral RNA probing, positions of cleavage were detected by primer extension with reverse transcriptase as previously described (Isel et al., 1995). The used primer was a 5′-end-labeled 18-mer oligodeoxyribonucleotide complementary to the PBS.

(–) strong stop DNA synthesis

RNA template (1 pmol) was annealed with 3′-end-labeled $tRNA_3^{Lys}$ (0.3 pmol) by heat or by NCp. Both $NCp_{(1–72)}$ and $NCp_{(1–55)}$ were used in this study. When $NCp_{(1–55)}$ was used, the NCp:RNA ratio was increased to one NCp per 5–6 nt. After proteinase K and phenol/chloroform treatment, 30 nM of primer/template complexes were incubated 4 min at 37 °C with 100 nM HIV-1 RT in 50 mM Tris-HCl, pH 8.0, 50 mM KCl, 6 mM $MgCl_2$, and 1 mM DTT. Reverse transcription was initiated by addition of the four dNTPs (50 μM final concentration each) and stopped with formamide containing 50 mM EDTA at times ranging from 15 s to 30 min. The reaction products were analyzed on 8% polyacrylamide denaturing gels and quantified with a BioImager BAS 2000 (Fuji).

ACKNOWLEDGMENTS

This work was supported by the Agence Nationale de Recherche pour le SIDA (ANRS). We thank D. Ficheux (Lyon) for gift of $NCp_{(1–55)}$, and C. Isel for useful discussions. F.B. was supported by fellowships from Sidaction and ANRS.

Received July 16, 2001; returned for revision September 12, 2001; revised manuscript received October 1, 2001

REFERENCES

Barat C, Lullien V, Schatz O, Keith G, Nugeyre MT, Grüninger-Leitch F, Barré-Sinoussi F, Le Grice SFJ, Darlix JL. 1989. HIV-1 reverse transcriptase specifically interacts with the anticodon domain of its cognate primer tRNA. *EMBO J 8*:3279–3285.

Baudin F, Marquet R, Isel C, Darlix JL, Ehresmann B, Ehresmann C. 1993. Functional sites in the 5′ region of human immunodeficiency virus type-1 RNA form defined structural domains. *J Mol Biol 229*:382–397.

Beerens N, Berkhout B. 2000. In vitro studies on tRNA annealing and reverse transcription with mutant HIV-1 RNA templates. *J Biol Chem 275*:15474–15481.

Beerens N, Klaver B, Berkhout B. 2000. A structured RNA motif involved in correct placement of the $tRNA_3^{Lys}$ primer onto the human immunodeficiency virus genome. *J Virol 74*:2227–2238.

Bénas P, Bec G, Keith G, Marquet R, Ehresmann C, Ehresmann B, Dumas P. 2000. The crystal structure of HIV reverse transcription primer tRNA(Lys,3) shows a canonical anticodon loop. *RNA 6*:1347–1355.

Cen S, Khorchid A, Gabor J, Rong L, Wainberg M, Kleiman L. 2000. Roles of Pr55gag and NCp7 in $tRNA_3^{Lys}$ genomic placement and the initiation step of reverse transcription in Human Immunodeficiency Virus Type 1. *J Virol 74*:10796–10800.

Chan B, Musier-Forsyth K. 1997. The nucleocapsid protein specifically anneals tRNALys-3 onto a noncomplementary primer binding site within the HIV-1 RNA genome in vitro. *Proc Natl Acad Sci USA 94*:13530–13535.

Chan B, Weidemaier K, Yip W-T, Barbara PF, Musier-Forsyth K. 1999. Intra-tRNA distance measurements for nucleocapsid protein-dependent tRNA unwinding during priming of HIV reverse transcription. *Proc Natl Acad Sci USA 96*:459–464.

Darlix JL, Lapadat-Tapolski M, de Rocquigny H, Roques BP. 1995. First glimpses at structure–function relationships of the nucleocapsid protein of retroviruses. *J Mol Biol 254*:523–537.

Das AT, Klaver B, Berkhout B. 1995. Reduced replication of human immunodeficiency virus type 1 mutants that use reverse transcription primers other than the natural $tRNA_3^{Lys}$. *J Virol 69*:3090–3097.

de Rocquigny H, Ficheux D, Gabus C, Fournie-Zaluski MC, Darlix JL, Roques BP. 1991. First large scale chemical synthesis of the 72 amino acid HIV-1 nucleocapsid protein NCp7 in an active form. *Biochem Biophys Res Comm 180*:1010–1018.

de Rocquigny H, Gabus C, Vincent A, Fournié-Zaluski MC, Roques B, Darlix JL. 1992. Viral RNA annealing activities of HIV-1 nucleocapsid protein require only peptide domains outside the zinc fingers. *Proc Natl Acad Sci USA 89*:6472–6476.

Feng YX, Campbell S, Harvin D, Ehresmann B, Ehresmann C, Rein A. 1999. The human immunodeficiency virus type 1 Gag polyprotein has nucleic acid chaperone activity: Possible role in dimerization of genomic RNA and placement of tRNA on the primer binding site. *J Virol 73*:4251–4256.

Guo J, Wu T, Anderson J, Kane BF, Johnson DG, Gorelick RJ, Henderson LE, Levin J. 2000. Zinc finger structures in the human immunodeficiency virus type 1 nucleocapsid protein facilitates efficient minus- and plus-strand transfer. *J Virol 74*:8980–8988.

Herschlag D. 1995. RNA chaperone and the RNA folding problem. *J Mol Biol 270*:20871–20874.

Huang Y, Khorchid A, Gabor J, Wang J, Li X, Darlix JL, Wainberg MA, Kleiman L. 1998. The role of nucleocapsid and U5 stem/A-rich loop sequences in tRNA(3Lys) genomic placement and initiation

of reverse transcription in human immunodeficiency virus type 1. *J Virol 72*:3907–3915.

Huang Y, Wang J, Shalom A, Li Z, Khorchid A, Wainberg MA, Kleiman L. 1997. Primer $tRNA_3^{Lys}$ on the viral genome exists in unextended and two-base extended forms within mature human immunodeficiency virus type 1. *J Virol 71*:726–728.

Isel C, Ehresmann C, Keith G, Ehresmann B, Marquet R. 1995. Initiation of reverse transcription of HIV-1: Secondary structure of the HIV-1 RNA/$tRNA_3^{Lys}$ (template/primer) complex. *J Mol Biol 247*:236–250.

Isel C, Lanchy JM, Le Grice SFJ, Ehresmann C, Ehresmann B, Marquet R. 1996. Specific initiation and switch to elongation of human immunodeficiency virus type 1 reverse transcription require the post-transcriptional modifications of primer $tRNA_3^{Lys}$. *EMBO J 15*:917–924.

Isel C, Marquet R, Keith G, Ehresmann C, Ehresmann B. 1993. Modified nucleotides of transfer-RNA_3^{Lys} modulate primer/template loop-loop interaction in the initiation complex of HIV-1 reverse transcription. *J Biol Chem 268*:25269–25272.

Isel C, Westhof E, Massire C, Le Grice SFJ, Ehresmann C, Ehresmann B, Marquet R. 1999. Structural basis for the specificity of the initiation of HIV-1 reverse transcription. *EMBO J 18*:1038–1048.

Kang SM, Zhang ZJ, Morrow CD. 1997. Identification of a sequence within U5 required for human immunodeficiency virus type 1 to stably maintain a primer binding site complementary to $tRNA^{Met}$. *J Virol 71*:207–217.

Krezel A, Lesniak W, Jezowska-Bojczuk M, Brasuñ J, Kozlowski H, Bal W. 2001. Coordination of heavy metals by dithiothreitol, a commonly used thiol group protectant. *J Inorg Biochem 84*:77–88.

Lanchy JM, Ehresmann C, Le Grice SFJ, Ehresmann B, Marquet R. 1996. Binding and kinetic properties of HIV-1 reverse transcriptase markedly differ during initiation and elongation of reverse transcription. *EMBO J 15*:7178–7187.

Le Grice SFJ, Grueninger-Leitch F. 1990. Rapid purification of homodimer and heterodimer HIV-1 reverse transcriptase by metal chelate affinity chromatography. *Eur J Biochem 187*:307–314.

Li XG, Mak J, Arts EJ, Gu ZX, Kleiman L, Wainberg MA, Parniak MA. 1994. Effects of alterations of primer-binding site sequences on human immunodeficiency virus type 1 replication. *J Virol 68*: 6198–6206.

Liang C, Li X, Rong L, Inouye P, Quan Y, Kleiman L, Wainberg MA. 1997. The importance of the A-rich loop in human immunodeficiency virus type 1 reverse transcription and infectivity. *J Virol 71*:5750–5757.

Mak J, Jiang M, Wainberg MA, Hammarskjöld M-L, Rekosh D, Kleiman L. 1994. Role of $Pr160^{gag\text{-}pol}$ in mediating the selective incorporation of $tRNA^{Lys}$ into human immunodeficiency virus type 1 particles. *J Virol 68*:2065–2072.

Marquet R, Baudin F, Gabus C, Darlix JL, Mougel M, Ehresmann C, Ehresmann B. 1991. Dimerization of human immunodeficiency virus (type 1) RNA: Stimulation by cations and possible mechanism. *Nucleic Acids Res 19*:2349–2357.

Mély Y, Cornille F, Fournié-Zaluski MC, Darlix JL, Roques BP, Gérard D. 1991. Investigation of zinc-binding affinities of Moloney murine leukemia virus nucleocapsid protein and its related zinc finger and modified peptides. *Biopolymers 31*:899–906.

Moine H, Ehresmann B, Ehresmann C, Romby P. 1997. Probing RNA structure and function in solution. In: Simons RW, Grunberg-Manago M, eds. *RNA structure and function*. Cold Spring Harbor, New York: Cold Spring Harbor Laboratory Press. pp 77–115.

Rein A, Henderson LE, Levin JG. 1998. Nucleic-acid-chaperone activity of retroviral nucleocapsid proteins: Significance for viral replication. *Trends Biochem Sci 23*:297–301.

Remy E, de Rocquigny H, Petitjean P, Muriaux D, Theilleux V, Paoletti J, Roques BP. 1998. The annealing of $tRNA_3^{Lys}$ to human immunodeficiency virus type 1 primer binding site is critically dependent on the NCp7 zinc fingers structure. *J Biol Chem 273*: 4819–4822.

Rong L, Liang C, Hsu M, Kleiman L, Petitjean P, de Rocquigny H, Roques BP, Wainberg MA. 1998. Roles of the human immunodeficiency virus type 1 nucleocapsid protein in annealing and initiation versus elongation in reverse transcription of viral negative-strand strong-stop DNA. *J Virol 72*:9353–9358.

Wakefield JK, Kang S-M, Morrow CD. 1996. Construction of a type 1 human immunodeficiency virus that maintains a primer binding site complementary to $tRNA^{His}$. *J Virol 70*:966–975.

Wakefield JK, Wolf AG, Morrow CD. 1995. Human immunodeficiency virus type 1 can use different tRNAs as primers for reverse transcription but selectively maintains a primer binding site complementary to $tRNA_3^{Lys}$. *J Virol 69*:6021–6029.

Williams MC, Rouzina I, Wenner JR, Gorelick RJ, Musier-Forsyth K. 2001. Mechanism for nucleic acid chaperone activity of HIV-1 nucleocapsid protein revealed by single molecule stretching. *Proc Natl Acad Sci USA 98*:6121–6126.

Zhang ZJ, Kang SM, Li Y, Morrow CD. 1998. Genetic analysis of the U5-PBS of a novel HIV-1 reveals multiple interactions between the tRNA and RNA genome required for initiation of reverse transcription. *RNA 4*:394–406.